




# Using Finite Element Modeling to Understand How Fish Resolve the 180° Ambiguity in Directional Hearing

Sujay Balebail, Vaibhav Chhaya, Johannes Veith,  
and Joseph A. Sisneros

## Contents

Introduction .....	2
Summary of Finite Element Models of Otolith Response to Sound in Fishes .....	4
Case Study: Finite Element Modeling of Swim Bladder Function in Directional Hearing of Female Plainfin Midshipman ( <i>Porichthys notatus</i> ) .....	5
Discussion and Conclusion .....	8
References .....	11

---

**OPEN ACCESS** with major support from 

---

S. Balebail (✉)

Département Adaptations du Vivant, Muséum National d'Histoire Naturelle, Paris, France

UMR MECADEV 7179 CNRS, Paris, France

e-mail: [balebail.sujay@mnhn.fr](mailto:balebail.sujay@mnhn.fr)

V. Chhaya

Department of Biology, University of Washington, Seattle, WA, USA

e-mail: [chhaya@uw.edu](mailto:chhaya@uw.edu)

J. Veith

Charité Universitätsmedizin Berlin, Berlin, Germany

Institut für Biologie, Humboldt-Universität zu Berlin, Berlin, Germany

e-mail: [johannes.veith@charite.de](mailto:johannes.veith@charite.de)

J. A. Sisneros

Department of Biology, University of Washington, Seattle, WA, USA

Department of Psychology, University of Washington, Seattle, WA, USA

Virginia Merrill Bloedel Hearing Research Center, University of Washington, Seattle, WA, USA

e-mail: [sisneros@uw.edu](mailto:sisneros@uw.edu)

© The Author(s) 2026

A. N. Popper et al. (eds.), *The Effects of Noise on Aquatic Life IV*,

[https://doi.org/10.1007/978-3-031-94229-7\\_21-1](https://doi.org/10.1007/978-3-031-94229-7_21-1)

---

**Abstract**

Fish detect sound primarily through particle motion, which creates a 180° ambiguity in determining sound direction. Some fishes with gas-filled structures closely associated with the inner ear such as the swim bladder can also sense acoustic pressure. Among these pressure-sensitive species, some have been shown to resolve this ambiguity by comparing the phase relationship between pressure and particle motion, which is opposite for sound arriving from opposite directions. However, the biomechanical basis by which these phase differences produce distinct motions of the otolith end organs remains unclear. To address this gap, finite element modeling was used to simulate motion of the right saccular otolith (RSO) in female plainfin midshipman (*Porichthys notatus*). Without a swim bladder, the RSO exhibited identical back-and-forth displacements at 100 Hz for sounds arriving from either side, preserving directional ambiguity. When the swim bladder was included, the RSO followed elliptical orbits whose handedness depended on sound direction. Reversing the phase relationship between acoustic pressure and particle motion also reversed handedness of RSO motion, effectively making the sound source appear to originate from the opposite direction. These results provide a mechanistic explanation for how swim bladders may enable fishes to resolve the 180° ambiguity in directional hearing.

---

**Keywords**

Swim bladder · Phase model · 180 ambiguity · Front-back ambiguity · Plainfin midshipman · FEM · Otolith · Sound localization

---

**Introduction**

The ability to determine sound direction serves important ecological functions such as detecting predators, finding food, and locating mates. Directional hearing has been demonstrated in some fish species, such as the Atlantic cod (*Gadus morhua*) (Buwalda et al. 1983) and the Ethereal danio (*Danionella cerebrum*) (Veith et al. 2024), and is likely present in many others.

Fishes possess two inner ears, one on each side of the brain, each containing three otolith end organs, the utricle, saccule, and lagena, as well as three semicircular canals. The semicircular canals are part of the vestibular system and detect angular acceleration (Highstein et al. 2005), whereas the otolith end organs contribute both to hearing and to vestibular function by detecting linear acceleration (Sand and Karlsen 2000). Each end organ contains a dense calcareous otolith coupled with a field of mechanosensory hair cells that form the sensory epithelium or macula (Sand et al. 2024) (Fig. 1). These hair cells are the auditory receptors. Relative motion between the otolith and the hair cell epithelium deflects the hair cell stereocilia and the kinocilium, altering cell polarity. This change modulates neurotransmitter release, which in turn adjusts the firing rate of postsynaptic auditory afferent fibers. These signals are then conveyed via the auditory nerve to the brain for further processing.

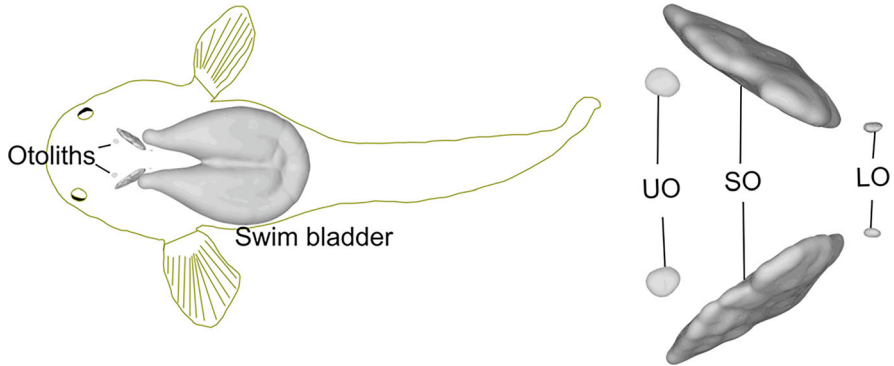


**Fig. 1** Left: Outline of a female plainfin midshipman fish (*Porichthys notatus*), showing the position of the inner ear otoliths and the swim bladder located adjacent to the inner ear. Right: Enlarged view of the three otoliths. UO indicates utricular otoliths (lapilli), SO indicates saccular otoliths (sagittae), and LO indicates lagenar otoliths (asterisci). (Copyright © 2025 Joseph Sisneros, all rights reserved)

Unlike terrestrial vertebrates, the inner ears of fishes primarily detect particle motion, the back-and-forth oscillation of acoustic particles within a sound field (Sand et al. 2024). Because fish tissues have acoustic impedances like that of water, sound propagates through the body with little change in direction. As a result, the inner ears oscillate with back-and-forth motion in line with the particle motion of the sound wave. This theoretically allows the hair cell populations to encode sound direction, as each hair cell exhibits directional sensitivity. However, this mechanism alone leads to a 180° ambiguity; a far-field sound source in front or behind the animal produces identical stimulation.

Nevertheless, evidence exists that some fishes resolve this ambiguity (reviewed in Veith et al. (2024), Supplementary Table 1). A proposed explanation for how fishes resolve the ambiguity is the phase model (Schuijf 1976), which posits that fishes distinguish between opposite directions by exploiting the phase relationship between particle motion and acoustic pressure. These two components are 180° out of phase for sounds arriving from opposite directions. For this mechanism to work, however, fishes must be able to detect acoustic pressure. In species with a gas-filled swim bladder that is either close to the inner ear or mechanically coupled to it, this is possible: the bladder expands and contracts in response to pressure fluctuations, converting pressure signals into local particle motion that can then be transmitted to the inner ear. In these species, otolith motion should include both (i) a direct component driven by incident particle motion and (ii) an indirect component derived from the pressure-induced swim bladder vibrations.

Resolving the 180° ambiguity, therefore, requires that otoliths move differently for opposite incident sound directions, producing distinct hair cell activation patterns. Testing this hypothesis requires comparing otolith motion in fishes with and without a functional gas-filled swim bladder. At biologically relevant sound levels, however, otolith displacements are only nanometers in scale (Sisneros and Rogers 2016), making direct experimental measurements technically challenging. Despite

advances in tomographic imaging and laser interferometry (Maiditsch et al. 2022; Veith et al. 2024), current techniques remain limited by measurement resolution and by the unnatural acoustic properties of small laboratory tanks, which differ markedly from natural open-water environments.

Mathematical modeling offers a powerful complement to these experimental challenges. Models allow researchers to probe how otoliths respond under controlled acoustic conditions, generate hypotheses about the role of ancillary structures such as the swim bladder, and guide the design of targeted experiments. Among modeling approaches, finite element modeling (FEM) has become particularly valuable for studying acoustic-structure interactions in biology. FEM discretizes complex geometries, such as otoliths, into a mesh of small polygonal or polyhedral elements connected at nodes. For fluid regions, the Helmholtz or linear wave equation is solved at the nodes, depending on whether the analysis is conducted in the frequency or time domain, while in solid regions, the Navier–Cauchy equation is applied. Interpolation functions then provide solutions across the entire structure.

In this chapter, existing FEM-based studies of fish otolith motion are reviewed, and a case study conducted on the plainfin midshipman fish (*Porichthys notatus*) is presented. The influence of the swim bladder on otolith kinematics is examined, and its potential role in resolving the 180° ambiguity in directional hearing is evaluated.

---

## Summary of Finite Element Models of Otolith Response to Sound in Fishes

Finite element models have provided important insights into how otoliths respond to sound and how accessory auditory organs, such as the swim bladder, influence otolith motion. Salas et al. (2019) studied larval red drum (*Sciaenops ocellatus*) and showed that the presence of a gas-filled swim bladder increased otolith acceleration in response to plane wave sounds across different frequencies. They also reported spatial variation in the response, with otolith regions positioned closer to the swim bladder experiencing greater acceleration than those farther away. Similar results were later observed in adult crucian carp (*Carassius carassius*) by Li et al. (2024). Zhang et al. (2021) focused on the yellow croaker (*Larimichthys crocea*) and calculated shear stress on the saccular otoliths. Their model revealed a peak at 800 Hz, within the species' most sensitive hearing range. Interestingly, shear stress was greatest when sound arrived perpendicular to the otolith surface, suggesting maximal saccular sensitivity to that orientation. This finding contrasts with experimental evidence indicating that saccules are generally most sensitive to sounds arriving parallel to the long axis of the saccular otoliths (Fay and Edds–Walton 2000), a discrepancy that requires further investigation. Wei and McCauley (2022) compared otolith responses in the bight redbelly (*Centroberyx gerrardi*) for sounds arriving from the front versus below the fish. They found that both acceleration and shear stress were greater for sounds from below. Collectively, FEM studies highlight two key conclusions: (i) the swim bladder can substantially amplify otolith motion, and (ii) otolith responses to sound are strongly direction-dependent, with both frequency and sound incidence angle shaping the mechanical output.

## Case Study: Finite Element Modeling of Swim Bladder Function in Directional Hearing of Female Plainfin Midshipman (*Porichthys notatus*)

The methods presented here will be described in greater detail in a forthcoming manuscript. Using COMSOL Multiphysics (v5.1.0.234), otolith motion in response to pure-tone, plane-wave sounds arriving from opposite directions was investigated, as well as the influence of the swim bladder on these dynamics in female plainfin midshipman. Otolith responses were also examined to determine whether they behave as if the sound originates from the opposite direction when the phase relationship between acoustic pressure and particle motion is inverted, providing a test of the phase model for resolving the 180° ambiguity. In the finite element models (FEMs), most fish tissues were assumed to have acoustic properties equivalent to water. The only structures modeled with distinct acoustic impedances were the six otoliths (two utricular, two saccular, and two lagenar) and the swim bladder.

The geometry of the swim bladder and otolith of a representative female plainfin midshipman was obtained via a CT scan acquired at 35.26 μm resolution (Skyscan 1076 microCT scanner, Bruker, Inc., USA). Otoliths and the swim bladder were segmented in 3D Slicer software (Fedorov et al. 2012) and exported as STL meshes. Because the swim bladder wall was not distinguishable in the CT images, a finite wall thickness was added using Meshmixer (Schmidt and Singh 2010). In the absence of measurements for plainfin midshipman, the swim bladder wall thickness of the closely related oyster toadfish (*Opsanus tau*; 824.5 μm; Fine et al. (2016)) was adopted. Instant Meshes (Jakob et al. 2015) was then employed to reduce mesh complexity so that FEM simulations in COMSOL could be run within memory limitations.

In order to simulate an open water environment, the mesh was imported into COMSOL and embedded within a water sphere (500 mm radius) centered on the geometry, and a spherical wave radiation boundary condition was assigned at the water sphere's surface, which allowed outgoing spherical waves to propagate without reflection. Finite element modeling of acoustic-structure interaction requires specification of material properties, namely density and the compressional ( $c_p$ ) and shear wave speeds ( $c_s$ ) of sound. Alternatively, in COMSOL, these properties can be defined using the material's Young's modulus ( $E$ ; the ratio of stress to strain) and Poisson's ratio ( $\nu$ ), the ratio of transverse strain (perpendicular to the applied force) to axial strain (parallel to the applied force). The corresponding wave speeds ( $c_p$  and  $c_s$ ) can then be derived from  $E$  and  $\nu$  using Eqs. (1) and (2):

$$c_p = \sqrt{\frac{E(1-\nu)}{\rho(1+\nu)(1-2\nu)}} \quad (1)$$

$$c_s = \sqrt{\frac{E}{2\rho(1+\nu)}} \quad (2)$$

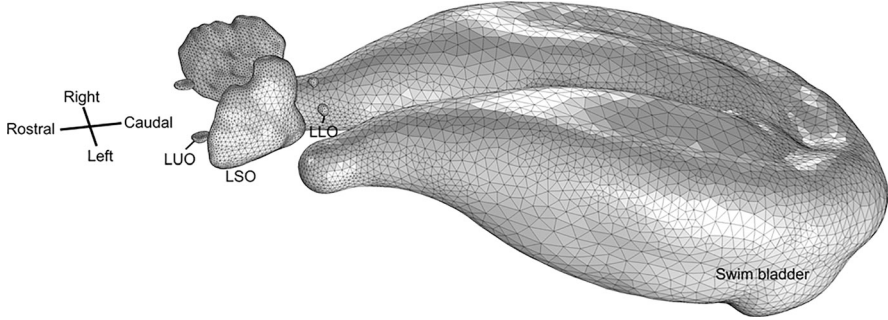


**Fig. 2** Mesh generated in COMSOL for the swim bladder and otoliths. LUO, LSO, and LLO stand for the left utricular, saccular, and lagenar otoliths, respectively. The surrounding water sphere (see text for details) was also meshed but is not shown. (Copyright © 2025 Joseph Sisneros, all rights reserved)

Thus, the pairs  $(c_p, c_s)$  and  $(E, \nu)$  provide equivalent information about material properties relevant to acoustic propagation. Soft tissues, such as the swim bladder wall, behave as damped oscillators (Fine et al. 2016); therefore, additional parameters are required to account for the damping of vibrations within this tissue.

Default acoustic properties for water were used (compressional wave speed,  $c_p = 1481$  m/s; density,  $\rho = 1000$  kg/m<sup>3</sup>). Otoliths were assigned the compressional and shear wave speeds of bone ( $c_p = 3000$  m/s,  $c_s = 1400$  m/s). Utricular and saccular otoliths, composed primarily of aragonite, were given a density of 2930 kg/m<sup>3</sup>, while the lagenar otoliths, composed of vaterite, were assigned a density of 2540 kg/m<sup>3</sup> (Li et al. 2024). The compressional and shear wave speeds of the swim bladder wall were estimated based on the density of water ( $\rho = 1000$  kg/m<sup>3</sup>), the Young's modulus ( $E = 1$  MPa) of the oyster toadfish swim bladder (Fine et al. 2016), and an estimated Poisson's ratio ( $\nu$ ) of 0.4999, typical of soft biological tissues whose  $\nu$  is nearly 0.5 (Fung 2013).

The air inside the swim bladder was assigned a density of 1.2 kg/m<sup>3</sup> and a  $c_p$  of 343.2 m/s, corresponding to COMSOL's default acoustic properties for air. The swim bladder wall was also assigned a shear viscosity of 2 Pa-s, representative of fish tissue (Khodabandeloo et al. 2021), to account for damping of its oscillations. Two geometries were created: one including both swim bladder and otoliths, and another with only otoliths (Fig. 2).

In the first set of simulations, a plane wave pressure field with a peak sound pressure level of 130 dB re 1  $\mu$ Pa was incident from either the left or right with respect to the fish. These simulations were performed for both geometries, with and without the swim bladder. Frequency-domain simulations were conducted for the swim bladder–otolith–water system at 100 Hz (Fig. 3).

Fluid regions, including the surrounding water sphere and the air bubble within the swim bladder, were modeled using the pressure acoustics, frequency-domain interface, which solves the Helmholtz equation to determine acoustic pressure. Solid regions, comprising the otoliths and swim bladder wall, were modeled with the solid

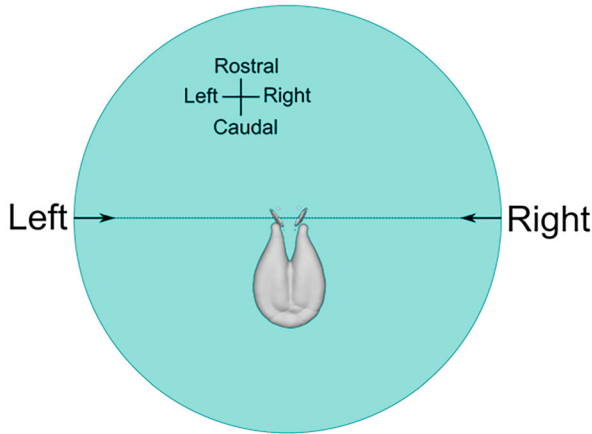
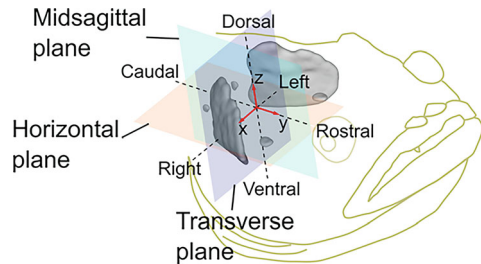


**Fig. 3** Finite element models were implemented where a pure tone, plane wave sound at 100 Hz was incident on either the swim bladder and otoliths, or just the otoliths from two opposite directions, left and right. The swim bladder and otoliths were positioned at the center of a large spherical water domain (shown as a blue circle; not to scale). A spherical radiation boundary condition was applied to the outer surface of the water domain to approximate an open-water acoustic environment (see main text for details). (Copyright © 2025 Joseph Sisneros, all rights reserved)

**Fig. 4** Local otolith-centered coordinate system to represent the motion trajectory of the center of mass of the right saccular otolith in response to incident sounds. (Copyright © 2025 Joseph Sisneros, all rights reserved)



mechanics interface, which applies the Navier–Cauchy equation in the frequency domain to calculate deformations caused by external forces and internal stresses. Boundaries between fluids and solids were treated as acoustic-structure interaction boundaries, where the acoustic pressure exerts forces on the solid domain, and the acceleration of the solid domain induces a normal acceleration in the adjacent fluid.

A local coordinate system was established with  $x$ ,  $y$ , and  $z$  axes corresponding to the rostral-caudal (R-C), mediolateral (left–right), and dorsoventral (D-V) directions, respectively (Fig. 4). One of the outputs of the COMSOL frequency-domain simulations is the amplitude and phase of displacement at each location in the solid domains. The amplitude and phase of displacement of the center of mass (COM) of the right saccular otolith along the  $x$  and  $y$  axes were extracted, and its motion in the horizontal plane was visualized by plotting  $u_t$  and  $v_t$ :

$$u_t = A_x \cdot \sin(2\pi f \cdot t + \Phi_x) \quad (3)$$

$$v_t = A_y \cdot \sin(2\pi f \cdot t + \Phi_y) \quad (4)$$

Here,  $u_t$  and  $v_t$  represent displacement in the  $x$  and  $y$  directions, respectively.  $A_x$  and  $A_y$  denote the amplitudes of displacement in the  $x$  and  $y$  directions, while  $\Phi_x$  and  $\Phi_y$  represent the corresponding phases. Time  $t$  ranges from 0 to 0.01 s, representing one time period ( $T = 0.01$  s), and was divided into 30 intervals of duration  $T/30$ . Custom MATLAB scripts were used to plot the otolith's COM-trajectory in the horizontal plane by visualizing  $u_t$  and  $v_t$  over one time period.

In simulations without the swim bladder, the right saccular otolith (RSO) moved back and forth identically for opposite sound directions (Fig. 5, top row). In contrast, with the swim bladder present, the RSO followed the same elliptical orbits in the horizontal plane for left- and right-incident sounds, but with opposite handedness: counterclockwise when viewed dorsally for sound from the left, and clockwise for sound from the right (Fig. 5, bottom row). Because hair cells are directionally sensitive, this difference in handedness likely produces distinct activation patterns in the hair cells, providing the brain with sufficient information to resolve these directions.

The phase model proposes that fish can resolve the  $180^\circ$  ambiguity by comparing the phase relationship between sound pressure and particle motion, which is inverted for opposite incident directions. To test this, otolith motion under inverted phase relationships between acoustic pressure and particle motion was examined. In the first simulation, a plane wave with a peak pressure amplitude of 3.16 Pa (130 dB re 1  $\mu$ Pa) was incident from the right. In the second simulation, three plane waves were incident on the swim bladder and otoliths: one from the left at 3.16 Pa, and two from dorsal and ventral directions at  $-3.16$  Pa, effectively inverting the phase of the pressure while leaving particle motion unchanged (Fig. 6). Similar sound configurations have successfully created directional hearing illusions in fish (Buwalda et al. 1983; Veith et al. 2024). Both simulations used a frequency of 100 Hz. Under phase inversion, the COM of the RSO moved along the same elliptical orbit with the same handedness as for the sound incident from the right. These results provide a biomechanical interpretation of the phase model, suggesting that when the phase relationship between acoustic pressure and particle motion is inverted, otoliths behave as if the sound is arriving from the opposite direction.

---

## Discussion and Conclusion

Simplified finite element models, which assumed that most fish tissues shared the acoustic properties of water and employed single-frequency plane-wave sound sources, indicated that the presence of a gas-filled swim bladder close to the inner ears can aid in resolving the  $180^\circ$  ambiguity in directional hearing at the peripheral auditory level. Specifically, the swim bladder induces elliptical otolith motion with

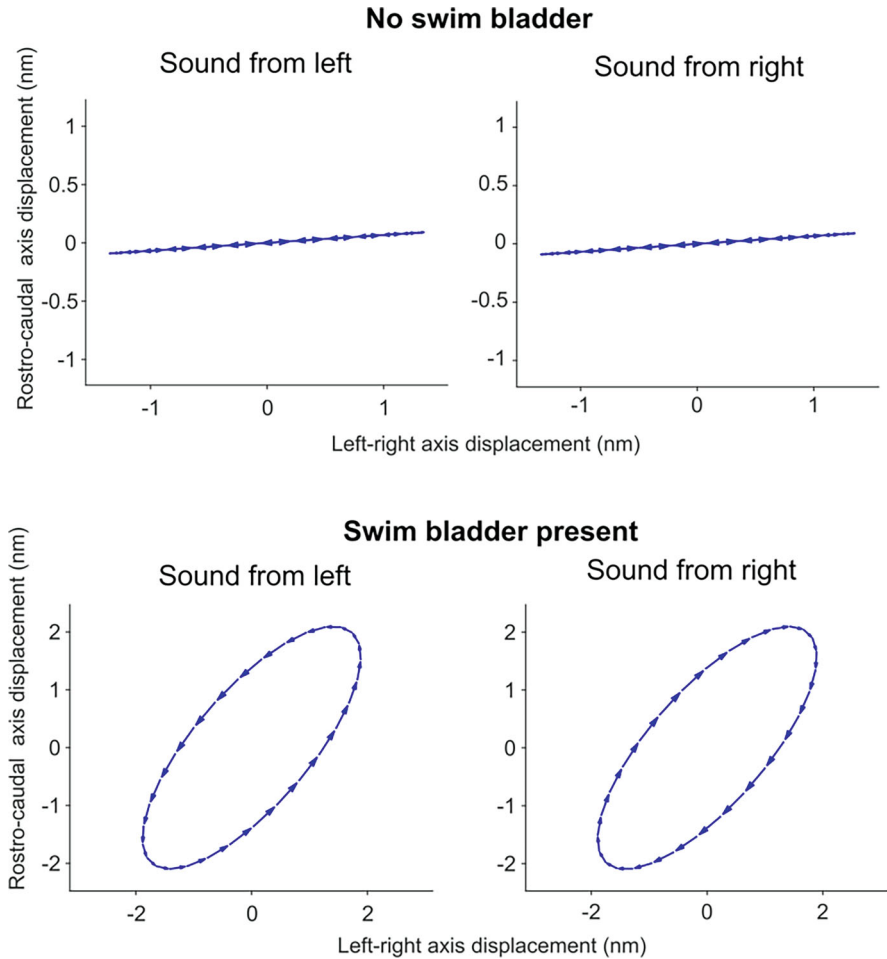


**Fig. 5** Center of mass displacements of the right saccular otolith in the horizontal plane in response to a 100 Hz plane wave. The left and right columns show sounds arriving from the left and right, respectively. The top row shows results in the absence of the swim bladder, while the bottom row shows results in the presence of the swim bladder. (Copyright © 2025 Joseph Sisneros, all rights reserved)

opposite handedness for sound arriving from opposing directions. The result provides a biomechanical basis for the phase model (Schuijff 1976), which proposes that fish resolve directional ambiguity by detecting phase differences between sound pressure and particle motion. In the simulations conducted, inverting the pressure-particle motion phase relationship caused the otoliths to move along trajectories identical to those produced by sound arriving from the opposite direction. Thus, the handedness of elliptical otolith orbits may encode the phase relationship, supplying

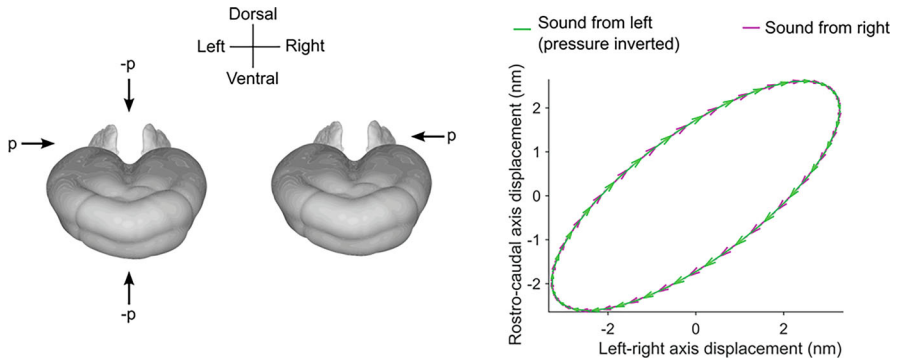


**Fig. 6** Horizontal-plane motion of the right saccular otolith's center of mass when a plane-wave sound arrived from the right, compared with the case in which sound arrived from the left at the same pressure amplitude ( $p$ ) and frequency (100 Hz). In the left-incident case, the phase relationship between pressure and particle motion was reversed by adding two vertically oriented (dorso-ventral) pressure fields with equal amplitude but opposite phase ( $-p$ ). (Copyright © 2025 Joseph Sisneros, all rights reserved)

the auditory system with cues to discriminate between front- and back-incident sounds.

This work is currently being extended to examine a broader range of sound directions, frequencies within the hearing range of the plainfin midshipman, sex-specific differences between type I males and females, and responses of all three otolith organs rather than just the saccule. A version of these extended findings is presented in Balebail (2024).

The findings of this study are consistent with the analytical modeling results of Schellart and De Munck (1987) who represented the swim bladder of cod as an oblate spheroid and demonstrated that particle motion followed elliptical orbits with opposite handedness for opposing sound directions. By incorporating realistic swim bladder geometry from CT scans and explicitly modeling the calcareous otoliths, which differ in acoustic impedance from water and likely shape local particle motion fields, the work of Schellart and De Munck (1987) has been built upon and extended. The consistency between the present results and those of Schellart and De Munck (1987) suggests that handedness-based encoding of elliptical otolith motion may represent a general mechanism for resolving directional ambiguity in fishes with swim bladders closely associated with or mechanically coupled to the inner ears.

Although sinusoidal plane wave inputs were the focus of this study, natural acoustic environments are considerably more complex and are characterized by non-sinusoidal waveforms and background ambient noise. It is unclear how the biomechanical mechanisms demonstrated in this study help resolve the  $180^\circ$  ambiguity for the diverse sounds that fish encounter in the wild. Veith et al. (2024) showed that *Danionella cerebrum* implement the phase model to resolve the  $180^\circ$  ambiguity for a non-sinusoidal sound, namely a complex transient sound (12 ms duration) with a center frequency of 780 Hz, suggesting that the phase model is

employed to resolve the 180° ambiguity for more complex sounds in this species, and possibly in other species in which the swim bladder is closely associated with the inner ears.

The frequency-domain analysis performed here can compute structural motion only for pure tones. However, FEM software such as COMSOL Multiphysics have the capabilities to perform time-domain analysis, in which the motion of structures (e.g., fish otoliths) can be computed as a function of time. Using this approach, more complex acoustic waveforms that resemble real-world sounds can be applied in future studies to examine otolith dynamics under ecologically relevant conditions and to determine whether the swim bladder also contributes to resolving directional ambiguities for biologically relevant stimuli.

Transient responses, such as the initial displacements that occur when sound first reaches the otoliths, were not addressed in the present simulations. Indeed, these transient dynamics may provide critical cues for directional hearing and sound source localization, including contributions to interaural time difference detection. These dynamics remain to be explored.

Finally, the present study emphasizes the swim bladder as the primary structure influencing otolith motion due to its distinct acoustic impedance relative to surrounding tissues. However, not all fishes possess gas-filled structures, and in many species possessing a swim bladder, the swim bladder is too far away from the otoliths to influence otolith motion. In fishes without a swim bladder, for example, flatfishes (Order Pleuronectiformes), other organs or tissues with contrasting acoustic properties may play analogous roles in shaping directional hearing. The modeling methodology presented here could be adapted to explore these possibilities. If the compressional and shear wave speeds, damping properties, and geometries of such tissues can be characterized, FEM can then be used to assess their contributions to auditory directionality.

**Competing Interest Declaration** The author(s) has no competing interests to declare that are relevant to the content of this manuscript.

---

## References

- Balebail S (2024) Decoding the information content of fish sounds and how fishes extract information from sounds: insights from the Plainfin midshipman and beyond. PhD Thesis, University of Washington
- Buwalda RJA, Schuijf A, Hawkins AD (1983) Discrimination by the cod of sounds from opposing directions. *J Comp Physiol* 150:175–184. <https://doi.org/10.1007/BF00606367>
- Fay RR, Edds-Walton PL (2000) Directional encoding by fish auditory systems. *Phil Trans R Soc Lond B* 355:1281–1284. <https://doi.org/10.1098/rstb.2000.0684>
- Fedorov A, Beichel R, Kalpathy-Cramer J et al (2012) 3D Slicer as an image computing platform for the Quantitative Imaging Network. *Magn Reson Imaging* 30:1323–1341
- Fine ML, King TL, Ali H et al (2016) Wall structure and material properties cause viscous damping of swimbladder sounds in the oyster toadfish *Opsanus tau*. *Proc R Soc B* 283:20161094. <https://doi.org/10.1098/rspb.2016.1094>

- Fung Y (2013) Biomechanics: mechanical properties of living tissues. Springer Science & Business Media
- Highstein SM, Rabbitt RD, Holstein GR, Boyle RD (2005) Determinants of spatial and temporal coding by semicircular canal afferents. *J Neurophysiol* 93:2359–2370. <https://doi.org/10.1152/jn.00533.2004>
- Jakob W, Tarini M, Panozzo D, Sorkine-Hornung O (2015) Instant field-aligned meshes. *ACM Trans Graph* 34:189–1
- Khodabandeloo B, Agersted MD, Klevjer TA et al (2021) Mesopelagic flesh shear viscosity estimation from in situ broadband backscattering measurements by a viscous–elastic model inversion. *ICES J Mar Sci* 78:3147–3161
- Li H, Gao Z, Song Z et al (2024) Investigation on the contribution of swim bladder to hearing in crucian carp (*Carassius carassius*). *J Acoust Soc Am* 155:2492–2502
- Maiditsch IP, Ladich F, Heß M et al (2022) Revealing sound-induced motion patterns in fish hearing structures in 4D: a standing wave tube-like setup designed for high-resolution time-resolved tomography. *J Exp Biol* 225:jeb243614
- Salas AK, Wilson PS, Fuiman LA (2019) Ontogenetic change in predicted acoustic pressure sensitivity in larval red drum (*Sciaenops ocellatus*). *J Exp Biol* 222:jeb201962
- Sand O, Karlsten HE (2000) Detection of infrasound and linear acceleration in fishes. *Phil Trans R Soc Lond B* 355:1295–1298. <https://doi.org/10.1098/rstb.2000.0687>
- Sand O, Popper AN, Hawkins AD (2024) Evolution of the understanding of fish hearing. In: Ketten DR, Coffin AB, Fay RR, Popper AN (eds) *A history of discoveries on hearing*. Springer International Publishing, Cham, pp 39–73
- Schellart NAM, De Munck JC (1987) A model for directional and distance hearing in swimbladder-bearing fish based on the displacement orbits of the hair cells. *J Acoust Soc Am* 82:822–829. <https://doi.org/10.1121/1.395280>
- Schmidt R, Singh K (2010) Meshmixer: an interface for rapid mesh composition. In: *ACM SIGGRAPH 2010 Talks*. ACM, Los Angeles, pp 1–1
- Schuijf A (1976) The phase model of directional hearing in fish. In: *Sound reception in fish*. Elsevier, Amsterdam, pp 63–86
- Sisneros JA, Rogers PH (2016) Directional hearing and sound source localization in fishes. In: *Fish hearing and bioacoustics: an anthology in honor of Arthur N Popper and Richard R Fay*, pp 121–155
- Veith J, Chaigne T, Svanidze A et al (2024) The mechanism for directional hearing in fish. *Nature* 631:1–7
- Wei C, McCauley RD (2022) Numerical modeling of the impacts of acoustic stimulus on fish otoliths from two directions. *J Acoust Soc Am* 152(6):3226–3234
- Zhang X-H, Tao Y, Zhou Y-L et al (2021) Acoustic properties of the otolith of the large yellow croaker *Larimichthys crocea* (Perciformes: Sciaenidae). *Zool Stud* 60:e64

**Open Access** This chapter is licensed under the terms of the Creative Commons Attribution-NonCommercial-NoDerivatives 4.0 International License (<http://creativecommons.org/licenses/by-nc-nd/4.0/>), which permits any noncommercial use, sharing, distribution and reproduction in any medium or format, as long as you give appropriate credit to the original author(s) and the source, provide a link to the Creative Commons license and indicate if you modified the licensed material. You do not have permission under this license to share adapted material derived from this chapter or parts of it.

The images or other third party material in this chapter are included in the chapter's Creative Commons license, unless indicated otherwise in a credit line to the material. If material is not included in the chapter's Creative Commons license and your intended use is not permitted by statutory regulation or exceeds the permitted use, you will need to obtain permission directly from the copyright holder.

